Gravel wash mud, a quarry waste material as supplementary cementitious material (SCM)

Vishojit Bahadur Thapa, Danièle Waldmann, Claude Simon

Vishojit Bahadur Thapa, Laboratory of Solid Structures, University of Luxembourg, L-1359 Luxembourg, Luxembourg

Danièle Waldmann, Laboratory of Solid Structures, University of Luxembourg, L-1359 Luxembourg, Luxembourg, Tel.: +352 46 66 44 5279, E-mail: daniele.waldmann@uni.lu

Claude Simon, Cimalux S.A., L-4002 Esch-sur-Alzette, Luxembourg

***Abstract* –** The suitability of gravel wash mud (GWM), a sludge waste from gravel quarrying, is examined for its use as a partial Ordinary Portland cement (OPC) clinker substitute. The gravel wash mud was dried, milled into a fine powder and calcined at 750°C, 850°C and 950°C. In this study, various characterisation methods including particle size distribution (PSD), X-ray fluorescence (XRF), X-ray diffraction (XRD) and the simultaneous thermal analysis (STA) were applied on the calcined GWM powders to determine the optimal calcination temperature. Over 200 specimens were prepared based on different cement paste and mortar mixes to investigate the potential of calcined GWM powders as SCMs. The pozzolanic activity of the GWM powders was verified by applying strength-based evaluation methods, simultaneous thermal analysis and SEM on hardened samples. Very promising strength-enhancing capacities were observed for samples containing GWM powders calcined at 850°C with a OPC replacement level of 20 wt.%.

***Keywords* -** Gravel wash mud (GWM), Supplementary cementitious materials, Alternative clay materials, Calcined clays, Pozzolanic activity.

1 Introduction

The inevitable CO_2 emissions related to cement manufacturing processes and its subsequent environmental impacts have received considerable critical attention worldwide and have become one of the key incentives for the development of environmental friendly and sustainable construction materials [1–3]. Furthermore, the growing demand for binders, mortars and concrete products opposed to the

increasing scarcity of raw materials for cement clinker production has imperatively stimulated the research on new binder technologies to assure the current and future demands for products based on cementitious materials [4–7]. Current trends in cement research have led to a large multitude of studies that suggest the partial substitution of OPC by admixtures, known as supplementary cementitious materials (SCM). Recent investigations and existing projects validate an important reduction of OPC usage by incorporation of SCMs in cement mixes [8] and the improvements of the final products' properties in contrast to the detrimental deteriorations of conventional concrete of aesthetical, functional or structural nature [9,10]. The beneficial effects of partial substitution of OPC by various SCMs on the packing of concrete mixtures, early hydration, mechanical performances and long-term durability have been extensively examined and confirmed. These improvements of mixture properties and performances due to addition of SCMs in cement-based mixtures can be attributed to three effects, which can occur simultaneously as coexisting processes or at distinctive stages over time [11–13]:

A) The chemical reaction: hydration of cementitious materials and pozzolanic reaction by formation of additional hydration products supplementary to the hydrated clinker phases [14–19].

B) The physiochemical impact: the finer particle size distribution of the added SCMs is correlated to larger contact surface area of the small particles, which provides larger interfacial area for the hydration reactions by performing as nucleation sites [20,21].

C) The physical effect: packing effect, respectively filler effect, leads to formation of a more effective and denser aggregate-cement paste matrix by filling the gaps between the cement particles themselves and between the cement particles and the aggregates [12,13,22–25].

Despite their high potentials and efficacy as partial OPC substitutes, the most commonly used SCMs like fly ash (FA) [26], silica fume (SF), ground granulated blast furnace slag (GGBS) and metakaolin (MK) are nowadays commercially available products and their prices have risen over the last decades due to growing demand. Thus, valuable and reliable research studies have been carried out on potential alternative SCMs and their performance as cement substitutes has been evaluated and studied mainly for local markets. The use of locally available resources as SCMs shows a considerable economical potential

as short transport routes as well as very low to no competitive price variations can be expected. Alternative SCMs comprise rice husk [27–29], industrially processed clays [30,31], calcined clay-brick wastes [32–35], volcanic tuffs [36,37], pumices [20], modified reservoir sludge [38–40], waste expanded perlite [41] and more [42–46].

Investigations on alternative SCMs using processed naturally occurring raw clay mixes and waste clay products have increased worldwide. This paper focuses on the potential of a quarry waste material, namely gravel wash mud (GWM), as SCM for partial substitution of OPC in cement-based mixes by presenting a variety of selected investigations including different material characterisation analyses and performance-based experimental tests. The main objective is to suggest an optimal OPC replacement level and to evaluate the mechanical performance of the novel cement-based products. Large series of mixtures were prepared, which consist of different cement paste and mortar mixes containing GWM powders calcined at 750°C, 850°C and 950°C.

The physical and chemical properties as well as the mineralogy of the GWM powders were evaluated using laser diffraction granulometry, the BET method, the X-ray fluorescence analysis, the quantitative X-ray diffraction analysis and the simultaneous thermal analysis (STA), which combines thermogravimetric analysis (TGA) and differential scanning calorimetry (DSC). Furthermore, the hardened specimens were analysed using compressive strength tests combined with performance-based evaluation methods, thermal analysis and scanning electron microscopy. The outcome of this study will enrich the investigations on waste materials as efficient alternative SCMs for OPC supplementation. Finally, the double benefit for society and industries consists of revalorizing an industrial waste product as SCM in cement mixes in an economically attractive and environmentally friendly way.

2 Materials and experimental program

2.1 Materials

The used Ordinary Portland cement (OPC) is a commercial CEM I 42.5 R cement (clinker content ≥ 95 wt.% according to EN 197-1 [47]) from Cimalux S.A, Luxembourg and a commercially available CEN-

standard sands was used for the OPC mortars, certified in accordance to EN 196-1 [48] with a characteristic grain size distribution with particle sizes ranging between 80 μm and 2 mm.

The gravel wash mud (GWM) was collected from a sandstone quarry in Folschette, Luxembourg operated by Carrières Feidt S.A. The raw mud was extracted from a settling pond and stored in sealed recipients. The water content of the sludge was 44 wt.% and 32 wt.%, in case a flocculation reagent was applied. The reddish brown mud-like deposit has a very plastic consistency. From geological point of view, the rock strata of the quarry consists of deposits of red sandstone. The GWM was desiccated at 105°C in a laboratory oven for two days. The dried GWM chunks were fragmented and ground into a powder, henceforth referred to as uncalcined GWM (UGWM) powder. The UGWM powder undergoes a thermal treatment procedure (calcination) to improve the reactivity of the aluminosilicates by dehydration and thermal decomposition (dehydroxylation) into a high-energy, amorphous raw material (CGWM). The calcination proceeded as follows: the powders were heated from room temperature up to the target temperature of 750°C, 850°C and 950°C at a heating rate of about 5°C/min in a laboratory chamber furnace with radiation heating (Model N41/H, Nabertherm GmbH, Germany). The peak calcination temperature was maintained for one hour and left for cooling down naturally to room temperature inside the chamber furnace.

2.2 Mixture preparation and mix proportion design

A large series of cement paste and mortar mixes corresponding to over 200 specimens were prepared to investigate the potential of CGWM powders as SCMs using the compressive strength of the hardened sample as indicator for the pozzolanic activity of the tested SCM, the optimal calcination temperature of the UGWM powders and the range of optimal OPC replacement level. Mix proportions of all studied mixes are summarized in **Table 1**. Nineteen different cement paste mixes (CG) including a control mixture and four different mortar mixes (CGS) including a reference mixture were prepared for curing times of 7, 28 and 56 days. The calcination time is fixed at 1h and the calcination temperature of the GWM powders was set at 750°C, 850°C and 950°C. The water/binder ratio was fixed to 0.4. For the binder mixes, the OPC substitution degree was varied from 5 wt.% up to 30 wt.% in steps of 5 wt.% and

the mortars were prepared at an arbitrarily fixed replacement level of 15 wt.% and a binder/aggregate (b/ag) ratio of 0.75.

The mixing procedure was kept constant for all the series of binder and mortar mixes, respectively. The quantities of Portland cement and calcined GWM powder were shortly dry-mixed at a mixing speed of 125 rpm. While keeping the same mixing speed, the water is gradually added and the compound is mixed for 180 seconds, followed by a final mixing at 250 rpm for 90 seconds. For the mortar mixes, the sand aggregates were added after the binder compound was mixed for 180 seconds, followed by mixing at 125 rpm and 250 rpm for another 90 seconds each. The specimens were cast in prismatic moulds (40 x 40 x 160 mm^3 according to EN 196-1 [48]) and compacted for 7 seconds on a vibrating table. After casting, the moulds were covered with plastic plates (5 mm thick) to prevent rapid loss of moisture and after 24 hours, the specimens were demoulded, wrapped in cellophane foil and cured at ambient temperature until 24 hours before the uniaxial compression tests according to [48].

Mixture*	**Calcination temperature CT** = 750°C / 850°C / 950°C; curing time of 7, 28 and 56 days**					
	Substitution degree	CGWM	OPC	CEN Sand	w/b***	b/ag****
[-]	[wt.%]	[g]	[g]	[g]	[-]	[-]
CG_R	0	0	425	-	0.40	-
CG_CT_5	5	21	404	-	0.40	-
CG_CT_10	10	43	383	-	0.40	-
CG_CT_15	15	64	361	-	0.40	-
CG_CT_20	20	85	340	-	0.40	-
CG_CT_25	25	106	319	-	0.40	-
CG_CT_30	30	128	298	-	0.40	-
CGS_R	0	0	225	180	0.40	0.75
CGS_CT_15	15	64	180	180	0.40	0.75

* Three specimens of each mixture were prepared for each curing time (7, 28, 56 and/or 90 days)
** e.g. CG_CT_5 series consists of mixtures CG_750_5, CG_850_5 and CG_950_5
*** w/b: water/binder ratio, binder equal to cement only or cement and CGWM
**** b/ag: binder/aggregate ratio

Table 1: Mix proportions of studied series of mixes

2.3 Experimental methods

2.3.1 Characterisation techniques applied on the primary powders and the hardened products

The laser diffraction method was used to determine the particle size distribution of the UGWM, CGWM

(750°C, 850°C and 950°C) and OPC powders. A modular particle size analyser (HELOS-RODOS-VIBRI, Sympatec GmbH, Germany) was utilised to measure the powder samples by dry powder dispersion using Fraunhofer diffraction theory [41] to compute the PSD from the diffraction patterns.

The characterisation of the specific surface area was performed on UGWM and OPC powders (two samples each) using the BET nitrogen gas adsorption method [42] according to ISO 9277:2010 [43], an extended method of the Langmuir monolayer molecular adsorption [44] to multiple molecular layers. The chemical composition of the powder samples was determined by X-ray fluorescence method using a wavelength dispersive X-ray fluorescence (WDXRF) spectrometer (S8 TIGER, Bruker AXS GmbH, Germany). The test specimens were prepared by pelletisation of the samples in a ring using the pressed powder technique.

The crystalline structure was investigated by quantitative X-ray diffraction analysis using a powder X-ray diffractometer using Cu-Kα radiation (D4 ENDEAVOR, Bruker AXS GmbH, Germany). The crystalline phases present in the GWM powders were identified by their characteristic d-spacings and intensities using the XRD software DIFFRAC.EVA (Bruker AXS GmbH, Germany). The X-ray diffraction patterns were processed using the program TOPAS (Bruker Corporation) using the fundamental parameter approach for line profile fitting [49] and the powder diffractograms were refined by the Rietveld method [50] after the crystalline phases were described using appropriate structural data from ICSD database.

Furthermore, the accurate and direct detection of non-crystalline matter in a powder sample is not possible with X-ray powder diffraction analysis, as those phases do not generate characteristic reflections peaks (X-ray amorphous). However, due to the likeliness of the presence of non-crystalline content (amorphous phases) in the GWM powders, its amorphous quantity is computed using quartz at 35% as an internal reference [64]. This procedure of quantitative phase analysis of amorphous content assumes that the internal reference quartz homogenously distributed within all powder samples, a narrow particle size distribution of all phases is ensured and a random orientation of the crystallites is assured to reduce preferred orientation effects [51, 64]. With the known amount of the internal reference W_{ref} and its

amount from the quantitative analysis W_q, the percentage of the amorphous content, $W_{amorphous}$, can be calculated as followed, adjusted from [51, 64]:

$$W_{amorphous} = 1 - \frac{W_{ref}}{W_q} \times 10^2 \ [\%]$$

Once the amorphous content is determined and with consideration of the known quantity of the internal reference, the sum of all phases is normalized to 100%.

Simultaneous thermal analyses (STA), a combination of thermogravimetric analysis (TGA) and differential scanning calorimetry (DSC), were performed on the GWM powder and the hardened cement-based binder. The applied thermo-analytical technique consists of the monitoring of the heat flow change and mass change of a sample as a function of temperature resp. time. The temperature was increased gradually from ambient temperature to 1000°C. The analysis of the STA curves permits the assessment of the nature of changes in the samples due to the increase of temperature and whether, the endothermic and exothermic effects occur with associated mass change corresponding to e.g. a melting effect or phase transition; or without mass change corresponding to e.g. degradation. The mineralogical analysis in combination with the STA data consists a great tool to determine the optimal calcination temperature and the phase shifts of the GWM powders and the hardened specimens.

2.3.2 Compressive strength test, relative strength test and pozzolanicity of the hardened binders

For each mixture, the compressive strength was measured on three specimens with same curing ages using a compression test plant (TONICOMP III, Toni Technik GmbH, Germany), conform to the standard DIN EN 196-1 [48], with additional displacement transducers. An indirect evaluation method of the pozzolanic activity, namely the strength activity index (SAI), is applied to measure physical properties of hardened test samples and to evaluate the magnitude of the pozzolanic activity [16,52–61]. In addition, a modified method is suggested for the determination of the level of pozzolanic reactivity of the calcined GWM powders. The proposed relative strength index (RSI) is based on the same principal as the strength activity index (SAI) using the ratio of the compressive strength of samples containing the

test pozzolan to the performance of a reference/control mixture as indicator for pozzolanic reactivity. However, the RSI method follows the hypothesis that if a tested material would not show any pozzolanic activity, neither any positive packing contribution nor reactivity to the cement matrix, then the expected loss in strength would be expected to be directly proportional to the substitution degree or higher. The RSP evaluation method directly provides information about the relative strength loss or gain of the pozzolanic material to a certain OPC substitution degree. The first step of the proposed evaluation (**Figure 1**) is to calculate the real potential (RP) which represents the ratio between the compressive strength of the specimens containing the test pozzolan and the control mixture. In case, the ratio is equal or above 100%, a net gain in strength was achieved from the substitution of OPC by calcined GWM powders. However, if RP value is below 100%, the consideration of the relative strength index (RSI), which is calculated by Eq. (1), provides an indication whether a relative strength gain, respectively loss occurred:

$$\mathrm{RSI} = \mathrm{RP} - (100\% - \mathrm{S}) \quad (1)$$

where RSI is the relative strength index, RP is the real potential (%), representing the ratio between the compressive strength of the specimens containing the test pozzolan and the control mixture, and *S* is the substitution degree of OPC by the SCM (%).

2.3.3 Microstructural characterisation of the cured binders

The microstructure of the hardened specimens was analysed using a high-resolution scanning electron microscope (LEO 440 REM, Carl Zeiss SMT AG, Germany). This SEM unit enabled high quality observations of structure surfaces down to 5 nm realised by detection of secondary backscattered electrons (BSEs) from a high-energy beam of primary electrons in a raster scan pattern. The preparation of small fractions of hardened material was performed after compression strength tests by gold coating. The images of the microstructure of selected samples were obtained by performing SEM on small fractions of the compressed specimens.

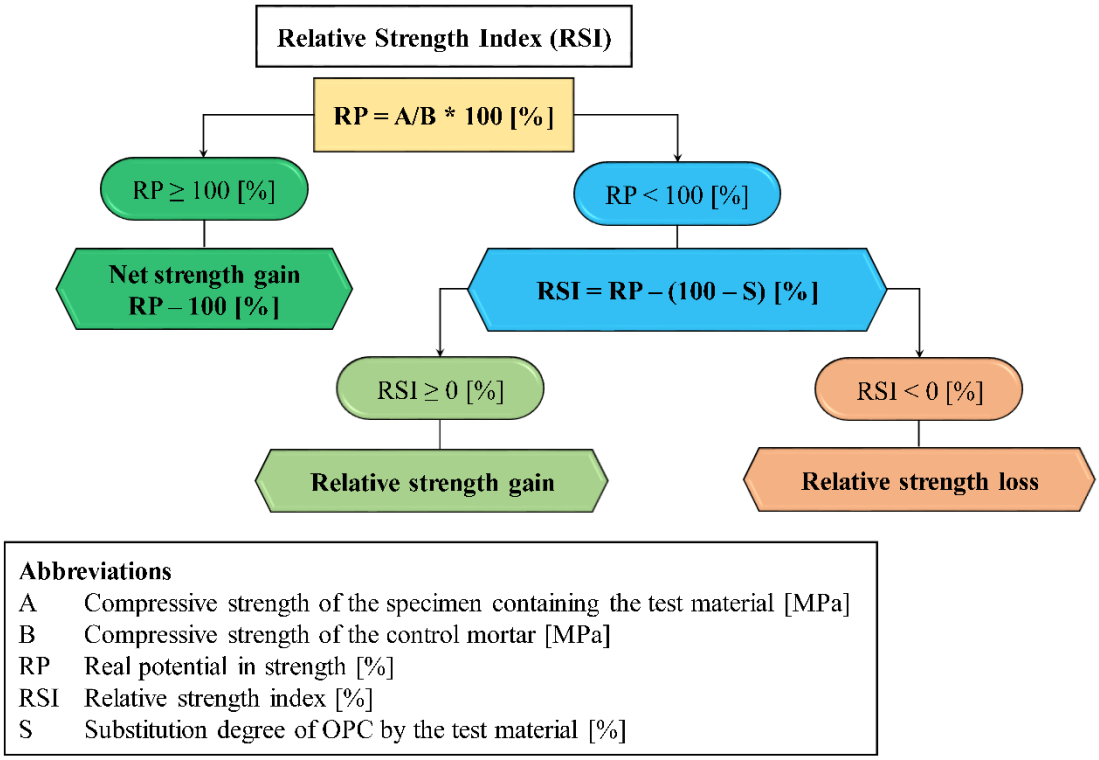

Figure 1: Relative strength index (RSI)

3 Results and discussions

3.1 Characteristics of the raw materials

3.1.1 Chemical analysis and PSD analysis

Figure 2 displays the PSD curves of UGWM, CGWM and OPC. The PSD analysis shows that the GWM powders present a very fine granulometry within a grain size range (d10-d90) from 1 to 35 µm with a mean particle size (d50) around 7-9 µm depending on the applied calcination temperature. CGWM powders at 850°C and 950°C have a slightly coarser distribution than UGWM and CGWM at 750°C due to the compaction of the minerals at high temperatures as a result of the sintering effect of clay particles [58, 59]. The OPC powder showed a specific surface area and a mean particle size of 436.50 m^2/kg and 11.58 µm, respectively. The aluminosilicate precursor UGWM showed a specific surface area of 522.49 m^2/kg with a mean particle size of 7.36 µm, whereas those for the CGWM powders, calcined at 750°C, 850°C and 950°C were 524.99 m^2/kg, 476.03 m^2/kg, 426.50 m^2/kg and 7.36 µm, 8.61 µm, 9.98 µm, respectively. The investigated CGWM powders show a finer grain size distribution than the

investigated cement powder, which forecasts an enhanced packing density of the mixes, already at small OPC substitution levels.

The chemical analysis (**Table 2**) confirms that the GWM is an aluminosilicate-rich material, which presents an elemental composition with high silica (SiO_2), medium alumina (Al_2O_3) and low iron oxide (Fe_2O_3) contents.

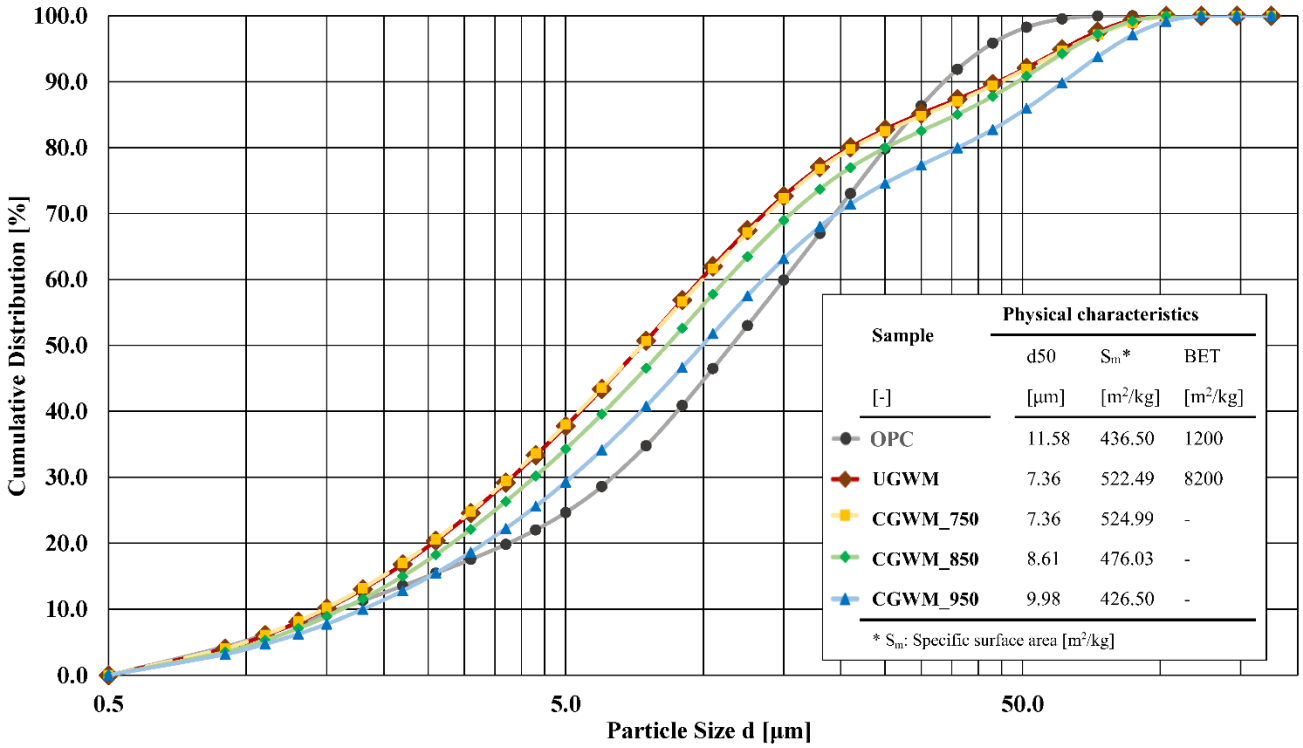

Figure 2: Particle size distribution and physiochemical characteristics of UGWM, CGWM (calcined at 750°C, 850°C and 950°C) and OPC powders

Sample	Chemical composition											
	SiO_2	Al_2O_3	Fe_2O_3	CaO	MgO	SO_3	Na_2O	K_2O	TiO_2	MnO	CeO_2	LOI
[-]	[%]	[%]	[%]	[%]	[%]	[%]	[%]	[%]	[%]	[%]	[%]	[%]
OPC	17.10	4.23	3.84	59.20	1.10	2.91	0.19	0.47	0.30	0.31	0.15	2.4
UGWM	52.30	15.70	7.53	0.33	1.34	0.07	0.19	2.19	0.69	0.05	-	-
CGWM_750	52.71	17. 26	8.51	0.22	1.14	0.07	0.23	3.08	0.75	0.08	-	-
CGWM_850	53.70	17.00	7.47	0.34	1.52	-	0.20	2.73	0.75	0.07	-	-
CGWM_950	53.93	17.45	7.87	0.22	1.34	0.04	0.25	3.11	0.63	0.08	-	-

Table 2: Chemical composition of UGWM, CGWM and OPC powders

3.1.2 X-ray diffraction (XRD) analysis a simultaneous thermal analysis (STA or TG-DSC)

Figure 3 illustrates the X-ray diffraction pattern of UGWM and the analysis reveals the presence of amorphous material, quartz, muscovite, illite, kaolinite, hematite and $KAl_3Si_3O_{11}$ in the GWM-based powders [40]. The quantitative analysis (**Table 3**), which was carried out based on the method described in [64], shows that the main crystalline phases identified were quartz, muscovite, followed by illite and kaolinite as clay minerals, hematite and the amorphous portions. The increase of the calcination temperature led to the transformation of the clay minerals into XRD amorphous phases. Two dehydroxylation phases can be pointed out with kaolinite entirely transformed to metakaolinite at temperatures below 750°C, whereas illite shifts towards amorphous phases above 850°C [40]. In addition, the quantity of muscovite is reduced above 750°C into a crystalline meta-phase, namely $KAl_3Si_3O_{11}$.

Figure 4 shows the curves of the STA analysis of the GWM powder, the mass loss (TGA) and the heat flow variation (DSC) of the GWM powder in function of the increase of temperature. The TGA curve shows two main phases of mass reduction (total: - 4.38%) of the investigated powder sample due to gradual increase of the applied temperature from ambient temperature up to 1000°C. The first gradual mass loss (- 0.96%) can be perceived from 30°C to around 350°C due to the evaporation of interlayer water of the aluminosilicate phases and the burning of organic matters or volatile components from the samples. The greater mass reduction (- 3.70%) occurs from about 350°C up to about 900°C mainly driven by the dehydroxylation of the clay minerals and further dehydration of structural water until a constant mass state is reached. The DSC curve confirms the burnout of the organic matter at about 300°C and the progressive dehydroxylation of the clay mineral phases from about 400°C to 550°C, followed by the phenomenon of quartz inversion (phase transition of quartz minerals) resulting in an endothermic peak at 575.3°C [65,66]. The findings of mineralogical analysis in combination with the STA suggest a primary indication of the optimum range of calcination temperature for the GWM powder at above 750°C as the loss in mass has more or less completed and the major phase shifts have occurred.

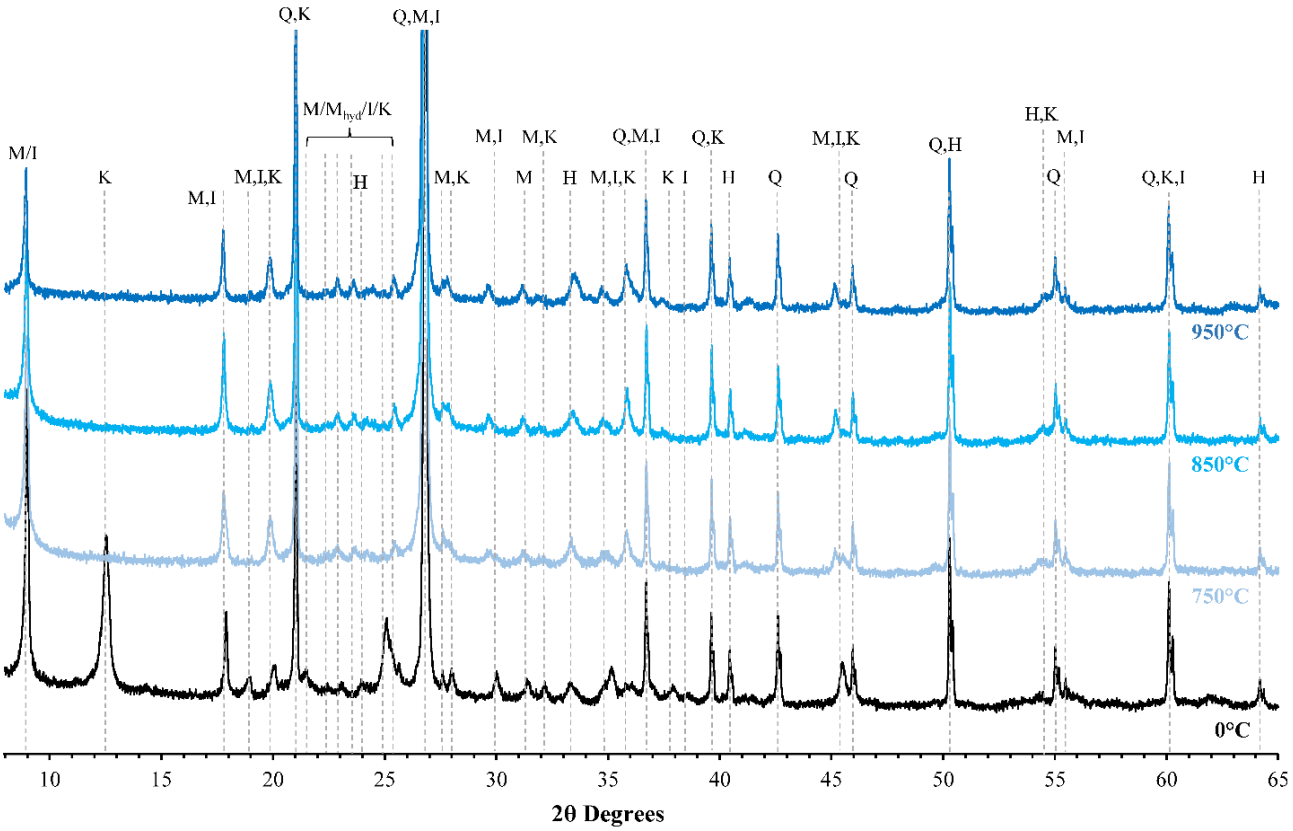

Figure 3: X-ray diffractogram of UGWM: Q - Quartz, M - Muscovite, I - Illite, K - Kaolinite, H - Hematite, M_{hyd} - $KAl_3Si_3O_{11}$

Sample	Mineralogical composition [%]							
	C_3S	C_2S	C_4AF	C_3A	Anhydrite	Calcite	Portlandite	Quartz
OPC	51.7	24.8	12.2	1.6	2.7	4.4	1.8	0.7
	Quartz*	Muscovite	Illite	Kaolinite	Hematite	$KAl_3Si_3O_{11}$	Amorph	
UGWM	35.0	16.5	13.2	11.3	0.6	1.5	21.9	
CGWM_750	35.0	9.3	13.8	0.4	2.0	8.3	31.1	
CGWM_850	35.0	8.7	12.4	0.3	2.1	7.2	34.4	
CGWM_950	35.0	3.6	8.9	0.5	2.5	6.6	42.9	

* Quartz content fixed for normalisation of data

Table 3: Mineralogical composition of UGWM, CGWM and OPC powders

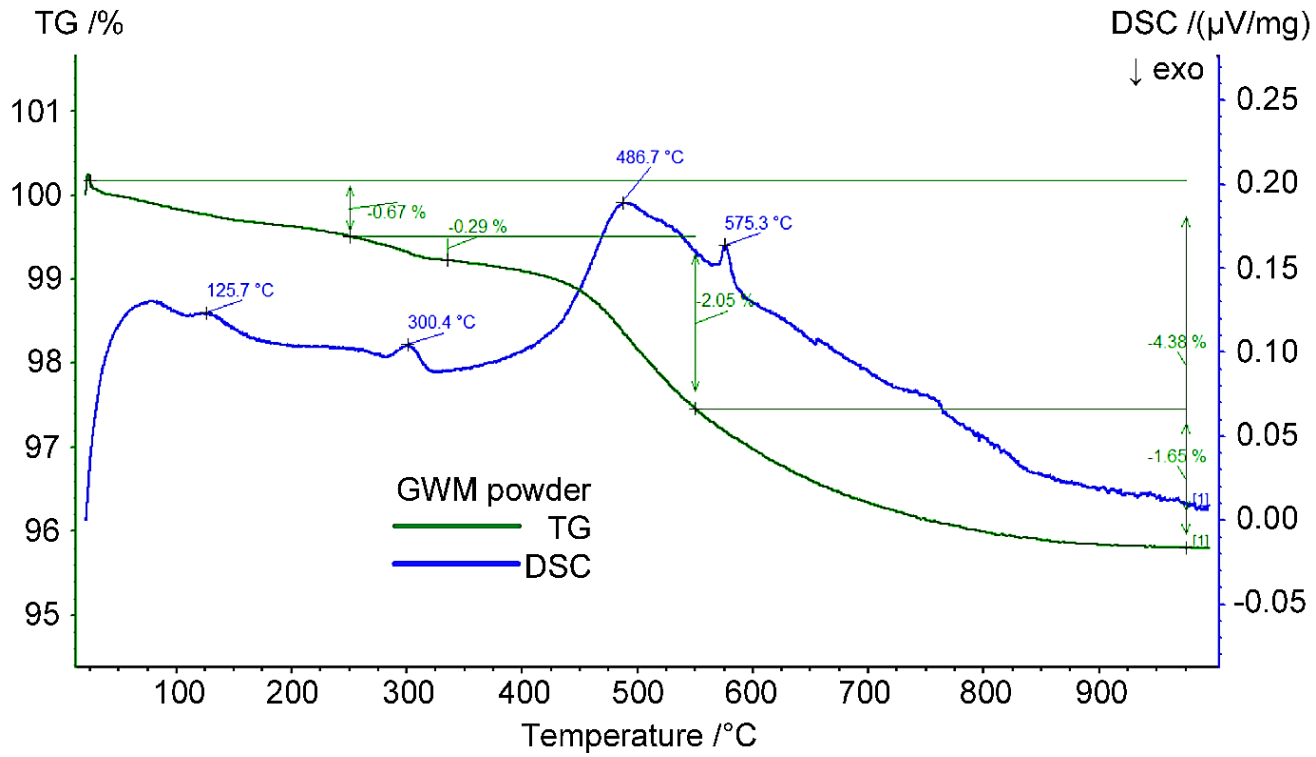

Figure 4: STA (TG-DSC) analysis of GWM powder

3.2 Characteristics of the hydrated specimens

3.2.1 Compressive strength tests of hardened specimens and pozzolanic activity

Figure 5-7 show the evolution of the compressive strength of hardened cement pastes containing different portions of GWM powders calcined at 750°C, 850°C and 950°C for up to 56 days of curing. Each compressive strength value represents the mean compressive strengths out of three valid specimen tests. All tested specimens showed a similar evolution of strength with a gain in compressive strength with increasing curing days. The progress of hydration of the cement clinker phases led to the formation of compact calcium silicate hydrates over the first days and months. With increasing curing ages, an additional increase in strength is considered for specimens containing CGWM powders due to the development of further reaction products from pozzolanic reaction. For example, an increase of 7.2 MPa from 28 days to 56 days of curing was observed for CG_850_15 compared to an increase of 3.5 MPa for the reference specimen over the same curing period. Moreover, an increase of the OPC replacement level by the CGWM powders, regardless the calcination temperature, did not result in a proportional loss in

strength of the hardened specimens after 28 resp. 56 days. Except at 7 days of curing, where a continuous loss of performance is observable with increasing quantity of CGWM powder. This phenomenon at early curing age can be related to the low reactivity of the CGWM powder and the fixed w/b ratio, which rather builds a physical obstruction for the clinker hydration reactions in the cement matrix than an enhancement due to pozzolanic reaction or better packing of the constituents. The development of the compressive strength at higher curing ages at 28 days and 56 days does not indicate a clear decline in compressive strength with increasing OPC substitution degrees. This suggests the formation of additional hydration products due to reactions between the CGWM powders and OPC, which is a strong indication for pozzolanic reaction. Furthermore, only the specimens containing GWM calcined at 750°C and 850°C showed an increase in strength from OPC replacement level of 15 wt.% up to 25 wt.% after 56 days of curing, whereas the development of compressive strength slightly declined for the specimens containing GWM powders calcined at 950°C. The highest compressive strengths at 56 days of curing were achieved for specimens CG_850_5, CG_950_5 and CG_850_10 with 53.97MPa, 53.07 MPa and 51.66 MPa respectively.

Hardened mortar mixes (**Figure 8**) containing GWM powders calcined at 750°C, 850°C and 950°C at an OPC replacement level of 15 wt.% showed similar compressive strength development over the investigated time period. The compressive strength of the hardened mortars CGS_850_15 exceeded the strength of the reference mortar at 28 days and 56 days and CGS_950_15 surpassed the reference compressive strength at 56 days. At early curing ages, the achieved compressive strength of the investigated mortars were inferior to the performances of the reference mortar. However, higher compressive strength values were realised at longer curing ages. The strength enhancement might be related to the pozzolanic reaction in combination with the formation of a denser microstructure due to a better cement paste distribution leading to an improved inter-aggregate bond compared to cement matrices without aggregates.

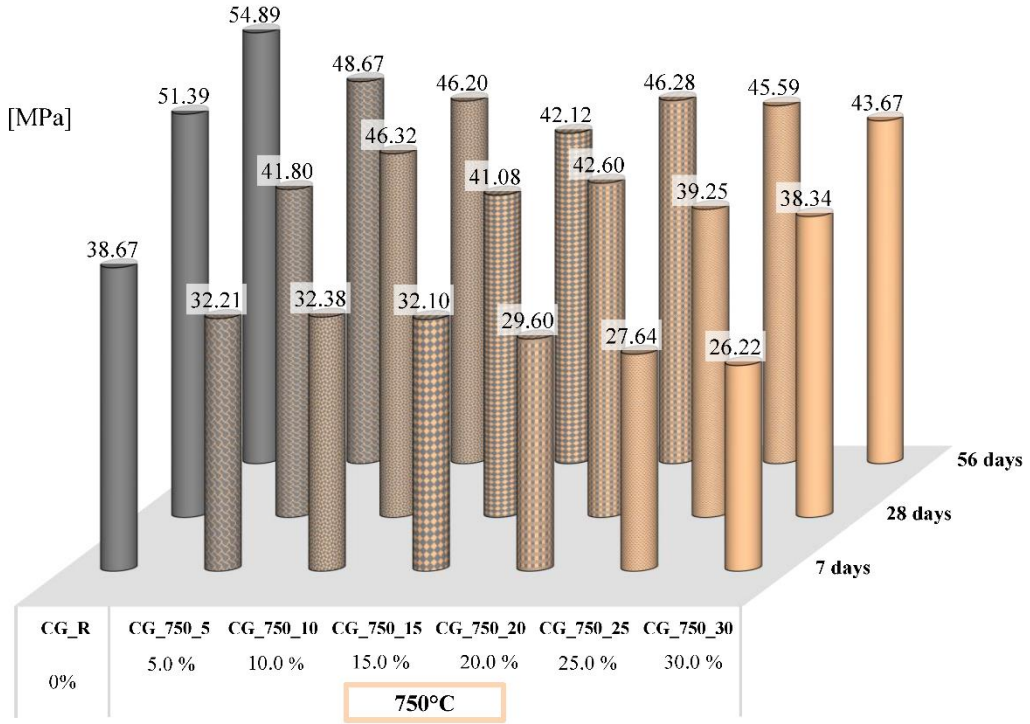

Figure 5: Development of the mechanical properties of hardened cement pastes containing CGWM (750°C) at different OPC substitution degrees

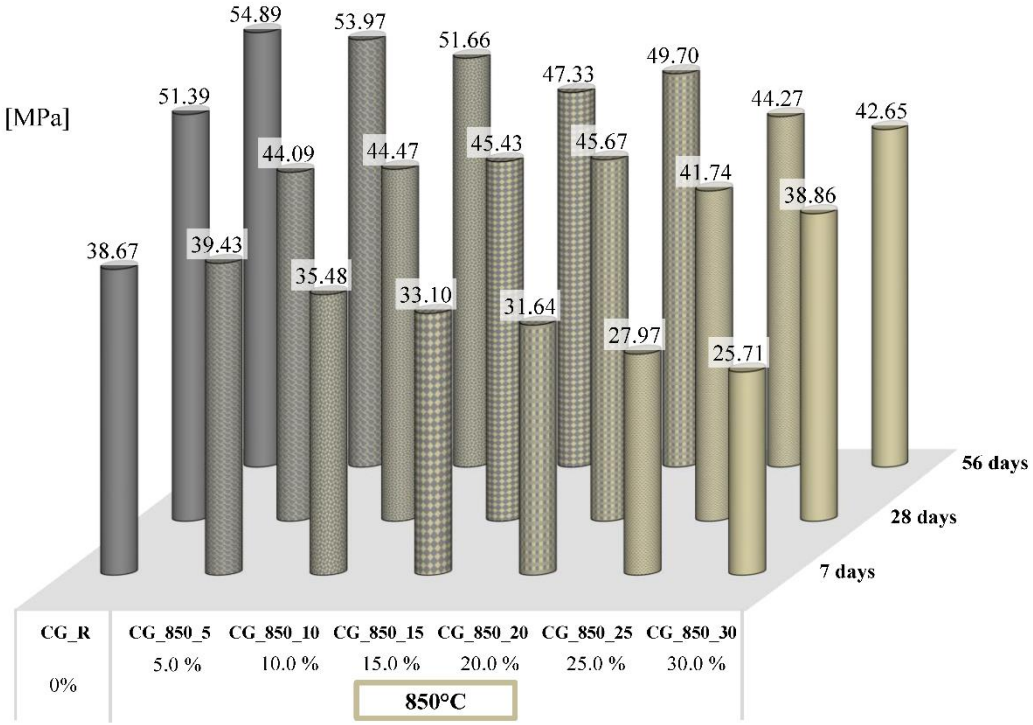

Figure 6: Development of the mechanical properties of hardened cement pastes containing CGWM (850°C) at different OPC substitution degrees

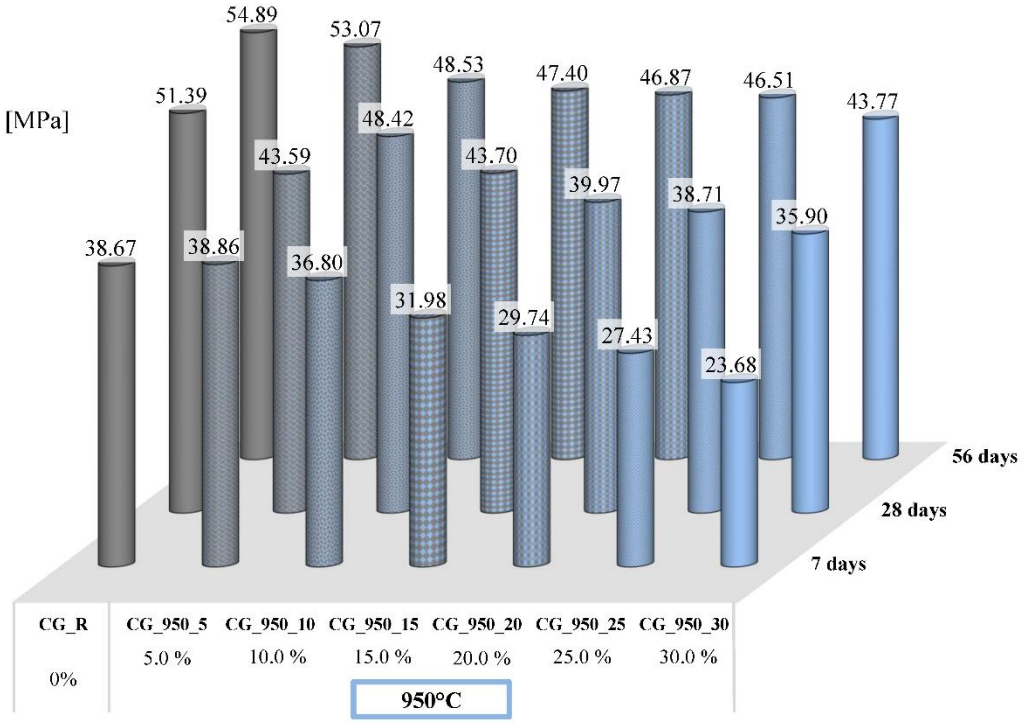

Figure 7: Development of the mechanical properties of hardened cement pastes containing CGWM (950°C) at different OPC substitution degrees

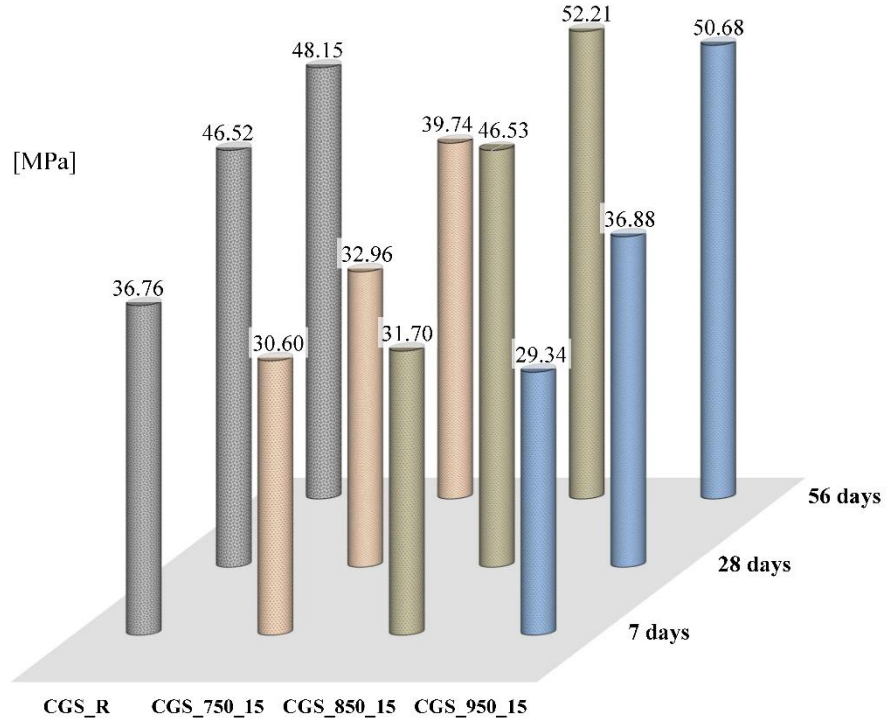

Figure 8: Development of the mechanical properties of hardened mortars containing different CGWM (750°C, 850°C and 950°C) at fixed OPC substitution degree of 15 wt.%

The direct comparison of absolute compressive strength is not sufficient to assess the pozzolanicity of CGWM at different calcination temperatures as well as the potential of the OPC substitution. Therefore, the strength activity index (SAI) method and the relative strength index (RSI) method are applied to

301 determine the optimal calcination temperature and the efficient OPC substitution degrees.
302 The chemical composition of the CGWM powders fulfils the physiochemical requirements on calcined
303 natural pozzolan according to specification in ASTM 618 [67] for usage as Portland cement admixtures.
304 The SAI were computed according to the test methods described in ASTM 311[68] for hardened cement
305 paste specimens containing CGWM powders (750°C, 850°C and 950°C) at the specified OPC
306 replacement level of 20 wt.% (**Figure 9**). The dashed line at 75% represents the minimal SAI according
307 to [68] on physical requirement on calcined natural pozzolans after 7 or 28 days of curing age. This
308 assessment enables to evaluate if the test pozzolan reaches an acceptable level of strength development
309 in a cement-based mixture, irrespective of whether the enhancement is from cementitious and/or
310 pozzolanic nature.
311 The strength activity indices of the evaluated cement pastes were above the requirement limit of 75 % at
312 all curing ages. The specimens containing GWM powders calcined at 850°C achieved the highest SAI of
313 81.8 %, 88.9 % and 90.5 % at 7, 28 and 56 days, respectively. The evaluation of the SAI confirms the
314 potential of the CGWM powders for strength developing properties as pozzolanic materials and indicates
315 that the optimal calcination temperature of the GWM powders is 850°C. However, the OPC replacement
316 level of 20 wt.% should be considered as a fixed evaluation parameter according to ASTM 311 [68]
317 rather than the recommended substitution amount of the test pozzolan. Therefore, the SAI method is
318 extended to all tested cement paste specimens for all investigated calcination temperatures, substitution
319 degrees and curing ages (**Figure 10-12**). The examination of the indices reveals that the strength
320 enhancement of specimens at OPC replacement level of 5 wt.% using GWM powders calcined at 850°C
321 and 950°C was led by the filler effect [12,13]. All samples with OPC substitution degrees from 5 wt.%
322 up to 20 wt.% fulfilled the minimal SAI requirements according to [61] for all investigated curing ages.
323 At curing age of 7 days (**Figure 10**), the specimens with a OPC replacement level above 25 wt.% did not
324 fulfil the minimal requirement, probably related to the dilution effect with increasing pozzolan content
325 which leads to an increased dispersion of cement particles and hence to a lower hydraulic reactivity.
326 **Figure 11** and **Figure 12** show that, with increasing curing age, most of the specimens with higher OPC

substitution degrees of 25-30 wt.% fulfil the minimal level of strength requirement as the pozzolanic reaction becomes more significant with development of additional CSH phases.

Figure 13 illustrates the calculated relative strength indices (RSI) of the hardened cement pastes after 56 days of curing age. The evaluation of the relative strength indices verify the previous analysis of the strength activity indices by showing a positive relative strength gain after 56 days of curing for the hardened cement pastes using higher OPC substitution degrees of 20-30 wt.% for all investigated calcination temperatures. The negative values for cement pastes using GWM powders calcined at 750°C at a replacement level from 5 to 15 wt.%,, respectively, at 950°C at a replacement level of 10 wt.% indicate a relative strength loss by taking into account the substitution degree and the performance of the reference samples. This relative strength loss expresses that at lower substitution degrees, the contribution from pozzolanic reaction to the (relative) strength gain of the cement pastes is lower than the strength development by cement hydration of the reference sample. The highest potential of relative strength gain is reached by the cement pastes containing GWM powders calcined at 850°C [69] at an optimal OPC replacement level of 20 wt.%.

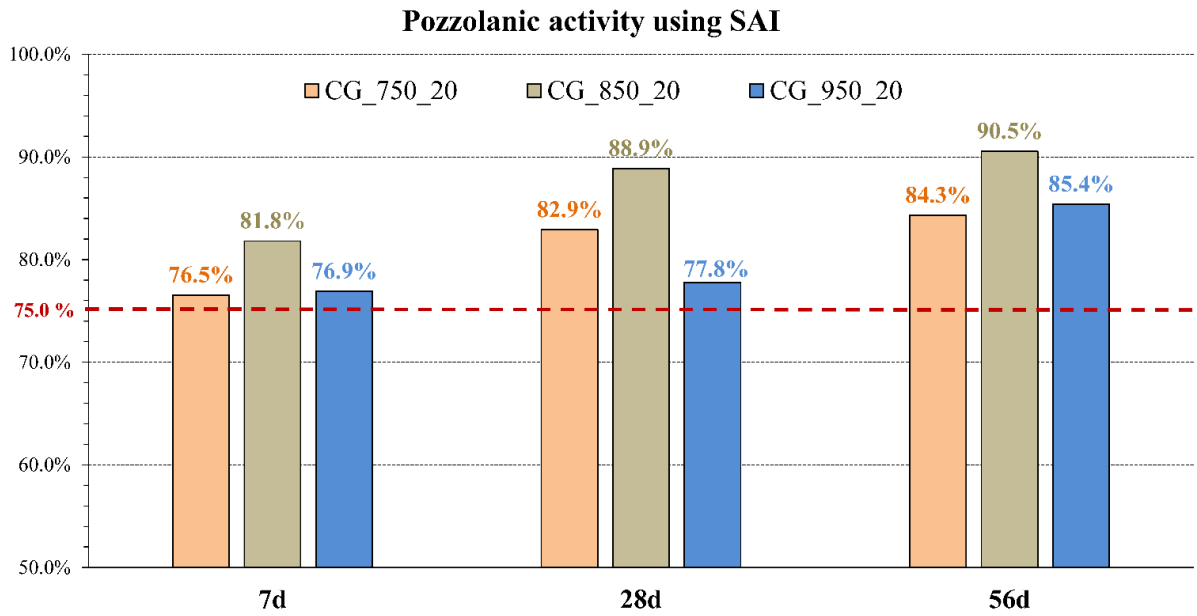

Figure 9: Strength activity indices of hardened cement pastes at OPC replacement level of 20 wt.% containing GWM powders calcined at 750°C, 850°C and 950°C; dashed line represents the limit for pozzolanic activity according to ASTM 618 [67]

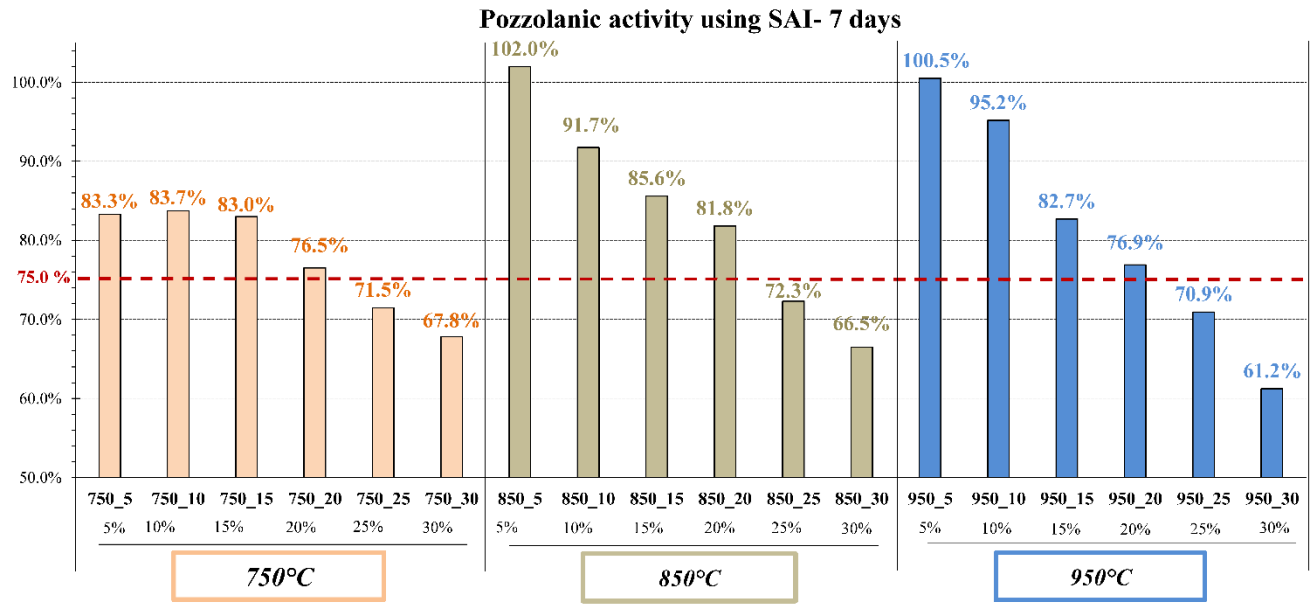

346

347 **Figure 10:** Strength activity indices of hardened cement pastes samples at 7 days of curing age

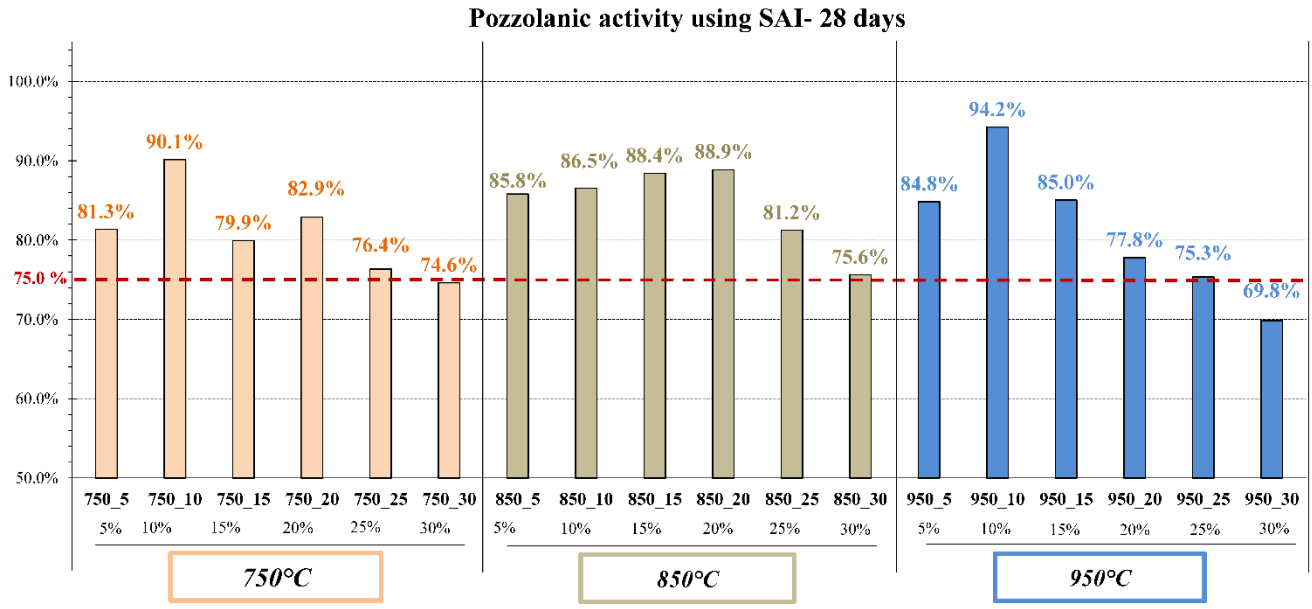

348

349 **Figure 11:** Strength activity indices of hardened cement pastes samples at 28 days of curing age

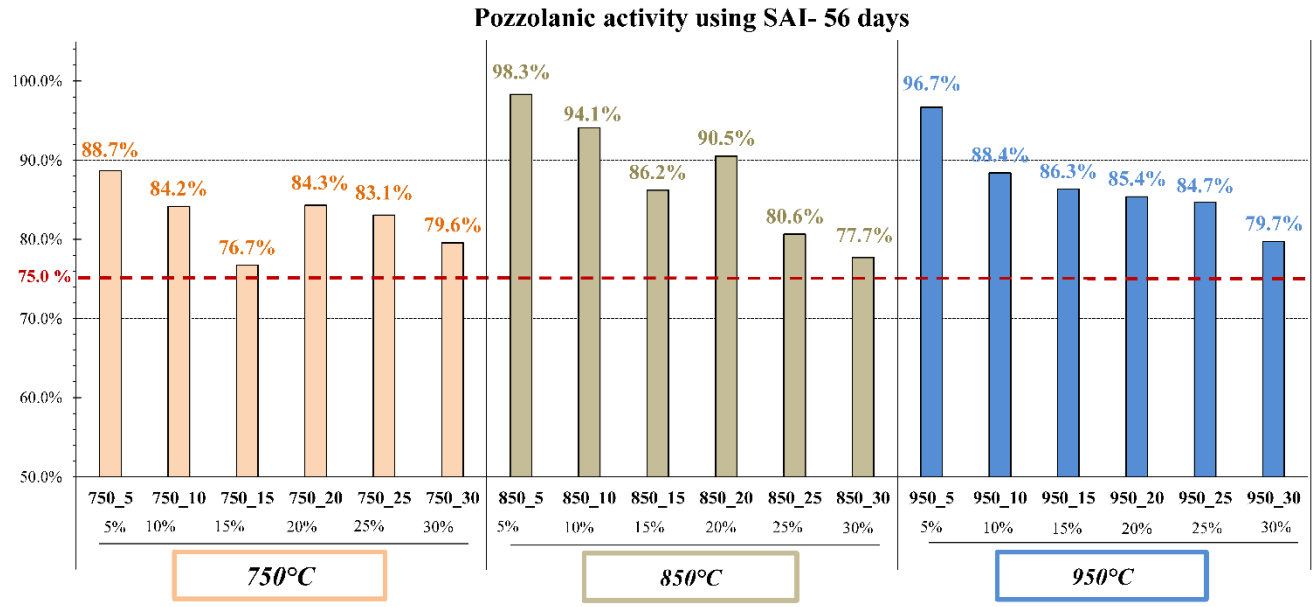

Figure 12: Strength activity indices of hardened cement pastes samples at 56 days of curing age

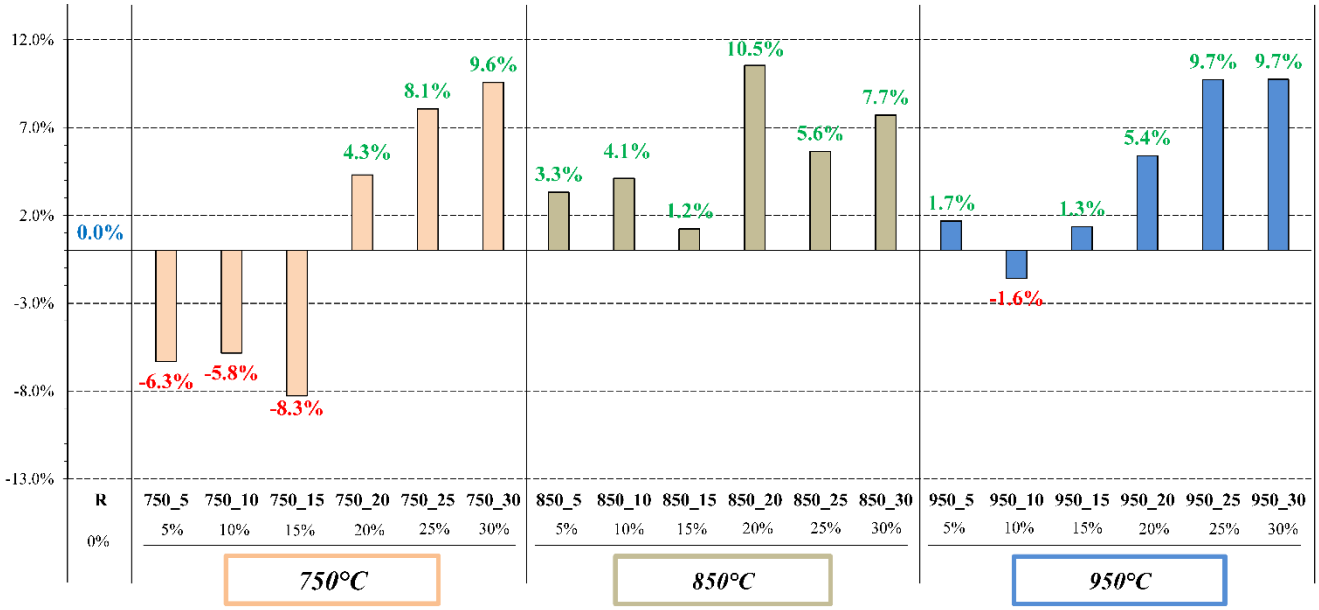

Figure 13: Evaluation of the mechanical performances (curing age of 56 days) of hardened cement pastes samples using the Relative Strength Index (RSI) method

3.2.2 Phase composition of the hardened specimens by STA

Figure 14 shows the results of STA of CG_850_20. The TGA curve (green) shows a total mass reduction of 21.83%, which can be divided in three stages: The first mass loss of 9.63% from room temperature up to 250°C occurs due to the heating of the clay minerals, leading to the evaporation of capillary pore water, interlayer water and absorbed water of the CSH phases in the system. The second mass loss of 4.66% is related to the dehydration of calcium hydroxide (Portlandite). The third loss in

mass of 7.54% from around 600°C up to 750°C can be attributed to the decarbonation of calcium carbonate ($CaCO_3$) in the binder system. Furthermore, the $CaCO_3$ carbonate results from the carbonation reaction of free Portlandite with CO_2 from air as no calcium carbonate was added in the initial mixture. The DSC curve approves the findings of the TG analysis and presents three ranges with endothermic peaks. The first peaks around 100°C and 150°C represents the dehydration process of the different hydration products and aluminosilicate minerals due to the evaporation of capillary pore water. The second endothermic peak around 450°C can be attributed to the dehydration of Portlandite. The final endothermic peaks observed between 700°C and 750°C correspond to the decarbonation of $CaCO_3$ [65, 66].

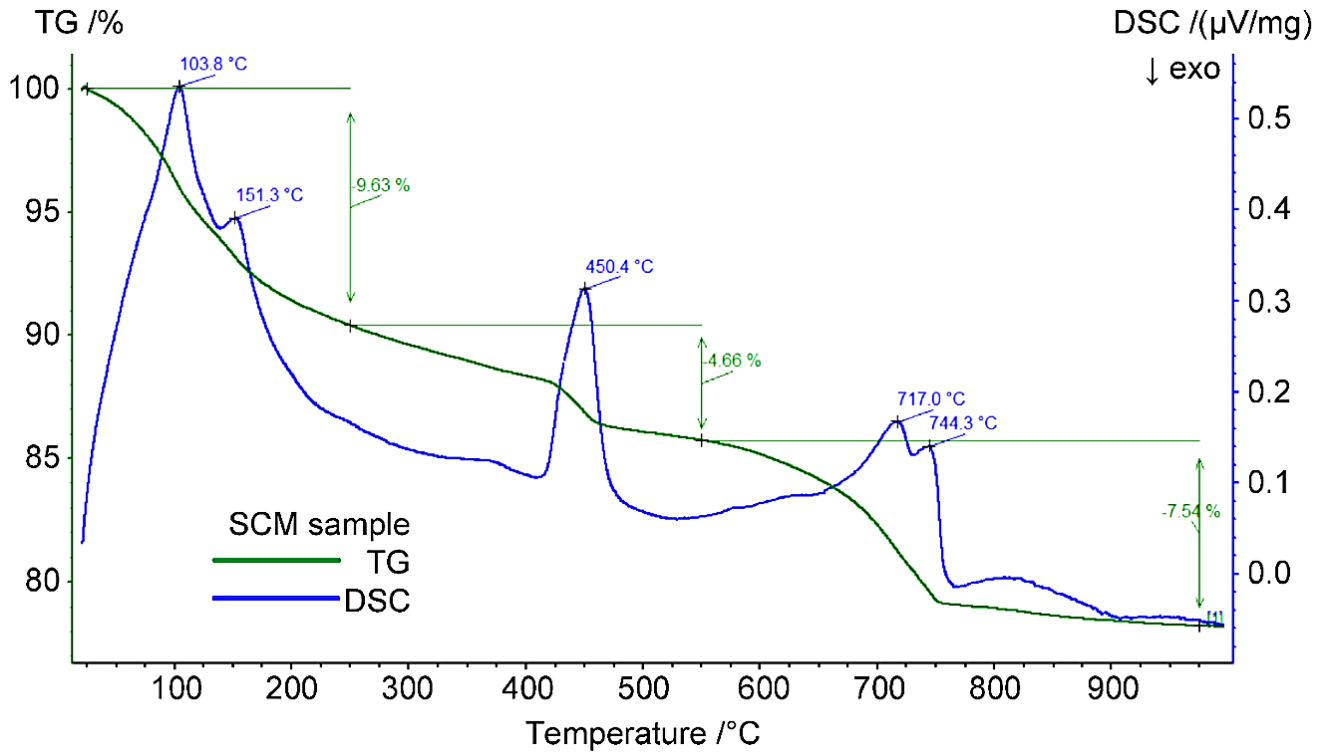

Figure 14: STA (TG-DSC) analysis of CG_850_20

3.2.3 Analysis of the microstructure

Figure 15a-c illustrates the images of the microstructure of hardened specimens after 56 days, which were captured by performing SEM on small fractions of the compressed specimens with different replacement levels of CGWM. **Figure 15a** depicts the SEM image of the control sample and the formation of a compact microstructure of calcium silicate hydrates with Portlandite crystals can be

observed with signs of local failures due to cracking of the hardened paste after the compression test. **Figure 15b** illustrates the microstructure of a hardened mixed paste with 20 wt.% of GWM powder calcined at 850°C. The bond between the hydrate phases and the amorphous cementitious formations results in a compact and dense microstructure. Some irregular cracks were also observed due to the fractioning of the samples. Despite the presence of local aluminosilicate agglomerates, consisting of unmixed/semi-mixed compounds, the hardened mix paste of specimens with low PC replacement level is homogenous and less porous than for specimens with higher substitution degrees due to a better packing of its constituents (filler effect) and a higher degree of cement hydration (**Figure 15c**). The microstructural analysis of the different samples verify that a compact microstructural composition between the aluminosilicate-rich compounds and the cement-based products was established. This bond suggests the development of pozzolanic reactions between the calcined GWM powders and OPC.

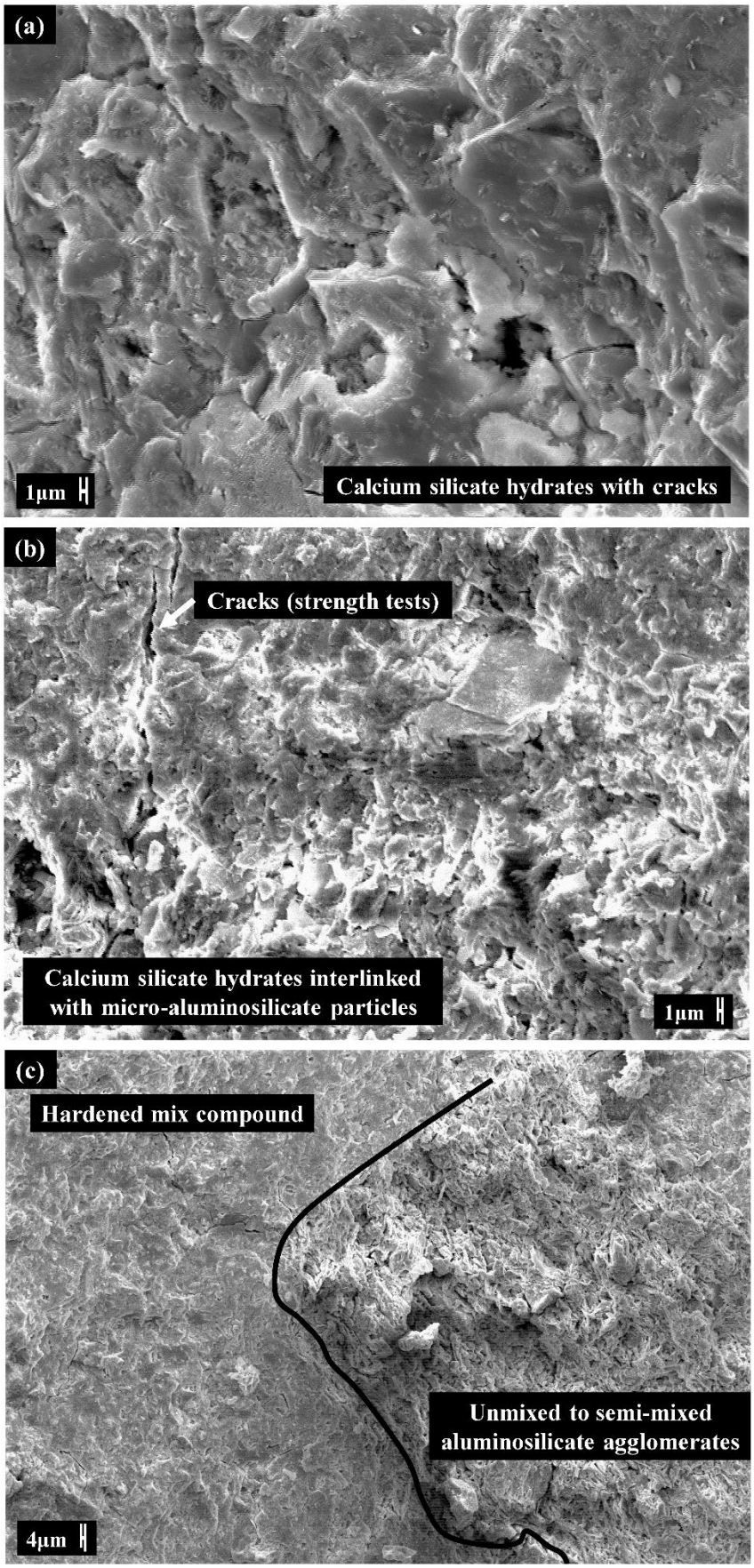

Figure 15: SEM images after 56 days of age: (a) reference mixture CG_R; (b) hardened mixtures CG_850_20; and (c) CG_850_5

4 Conclusions

In the present study, gravel wash mud (GWM) powder, an aluminosilicate prime material, derived from a waste sludge from gravel quarrying and after undergoing a calcination process, was evaluated as a novel supplementary cementitious material. From the findings of the different investigations, the following conclusions can be drawn:

- The studied GWM powders are fine aluminosilicate-rich materials with a mean particle size around 7-9 μm depending on the applied calcination temperature. The mineralogy is mainly composed of quartz, illite and kaolinite as clay minerals, muscovite, hematite and a high amorphous portion.
- The evaluation of the mineralogy in combination with the STA analysis indicates that the increase of the calcination temperature led to the transfer of the clay phases into reactive hydrous and amorphous phases and therefore suggests the optimum calcination temperature for the GWM powders to be ranged above 750°C.
- The mechanical strength-based evaluation methods, the SAI and RSI methods applied on all investigated specimens, confirmed the pozzolanic activity of the CGWM powders.
- OPC substitution degrees ranging from 5% up to 25% by calcined GWM powders led to the development of a reliable, well-performing hardened cement paste/mortar products.
- The highest compressive strengths were achieved for specimens CG_850_5, CG_950_5 and CG_850_10 with 53.97MPa, 53.07 MPa and 51.66 MPa, respectively. However, the highest strength-enhancing potential regarding the mixing proportions and relative strength gain was observed for the samples containing GWM powders calcined at 850°C for one hour with a OPC replacement level of 20 wt.%. A pozzolanic composite cement of CEM II/A-Q or CEM II/B-Q, standardized according to EN 197-1 [47] could be a medium-term option for the use of the calcined GWM powders.
- The associated environmental and economic benefits favour the use of CGWM powders as OPC substitution: The CO_2 emissions related to the calcination process of GWM powder (850°C) is

lower than for the sintering (1450°C) of the prime materials during the production of Ordinary Portland cement. In addition, the waste material is no longer uneconomically landfilled due to its revalorisation as a partial OPC substitute. Nonetheless, further optimization are required, namely on the on-site removal of excess water of wet GWM to avoid extra transport costs if a practicable industrial usage of GWM is intended. From an environmental point of view, if compared directly with the range of different raw materials used to produce cement clinker, the environmental benefit of using GWM or similar industrial waste materials is evident considering the usage of a waste product and consequently the reduced depletion of limited natural resources required for cement clinker production.

This study confirms the pozzolanic activity of calcined GWM material as well as its strength-enhancing properties as filler material leading to higher compressive strengths for cementitious mixtures already at lower OPC substitution degrees. Even though promising results were obtained, further research on large-scale raw material processing, optimization of the mixing proportions, the study of the rheology, durability and other properties of fresh and hardened concrete mixture containing calcined GWM powders as alternative SCM, need to be carried out to implement a sustainable concrete product with a low carbon footprint for constructive applications.

5 Acknowledgements

The authors would like to express their gratitude to Carrières Feidt S.A. to have kindly supplied the gravel wash mud (GWM) used in this work and Cimalux S.A. with its partner institution Wilhelm Dyckerhoff Institut (WDI), particularly to Dr. Marcus Paul, for their expertise and helpful contributions to the material characterisation.

Bibliography

[1] J. Ke, M. Mcneil, L. Price, N.Z. Khanna, N. Zhou, Estimation of CO2 emissions from China's cement production: Methodologies and uncertainties, 57 (2013) 172–181. doi:10.1016/j.enpol.2013.01.028.

[2] E. Benhelal, G. Zahedi, E. Shamsaei, A. Bahadori, Global strategies and potentials to curb CO2 emissions in cement industry, J. Clean. Prod. 51 (2013) 142–161. doi:10.1016/j.jclepro.2012.10.049.

[3] W. Shen, L. Cao, Q. Li, W. Zhang, G. Wang, Quantifying CO2 emissions from China's cement industry, Renew. Sustain. Energy Rev. 50 (2015) 1004–1012. doi:10.1016/j.rser.2015.05.031.

[4] N. Li, D. Ma, W. Chen, Projection of cement demand and analysis of the impacts of carbon tax on cement industry in China, Energy Procedia. 75 (2015) 1766–1771. doi:10.1016/j.egypro.2015.07.457.

[5] Y. Cancio, U. Heierli, A.R. Favier, R.S. Machado, K.L. Scrivener, J. Fernando, M. Hernández, G. Habert, Limestone calcined clay cement as a low-carbon solution to meet expanding cement demand in emerging economies, 2 (2017) 82–91. doi:10.1016/j.deveng.2017.06.001.

[6] K. Scrivener, F. Martirena, S. Bishnoi, S. Maity, Calcined clay limestone cements (LC3), Cem. Concr. Res. 114 (2017) 49–56. doi:10.1016/j.cemconres.2017.08.017.

[7] F. Avet, K. Scrivener, Investigation of the calcined kaolinite content on the hydration of Limestone Calcined Clay Cement (LC3), Cem. Concr. Res. 107 (2018) 124–135. doi:10.1016/j.cemconres.2018.02.016.

[8] K.L. Scrivener, V.M. John, E.M. Gartner, Eco-efficient cements: Potential economically viable solutions for a low-CO2cement-based materials industry, Cem. Concr. Res. 114 (2018) 2–26. doi:10.1016/j.cemconres.2018.03.015.

[9] Portland Cement Association, Types and Causes of Concrete Deterioration, PCA R&D Spec. N. 2617. (2002) 1–16.

[10] Y. Farnam, B. Zhang, J. Weiss, Evaluating the use of supplementary cementitious materials to mitigate damage in cementitious materials exposed to calcium chloride deicing salt, Cem. Concr. Compos. 81 (2017) 77–86. doi:10.1016/j.cemconcomp.2017.05.003.

[11] A. Goldman, A. Bentur, The influence of microfillers on enhancement of concrete strength, Cem. Concr. Res. 23 (1993) 962–972.

[12] G.C. Isaia, A.L.G. Gastaldini, R. Moraes, Physical and pozzolanic action of mineral additions on the

mechanical strength of high-performance concrete, Cem. Concr. Compos. 25 (2003) 69–76. doi:10.1016/S0958-9465(01)00057-9.

[13] H. Moosberg-Bustnes, B. Lagerblad, E. Forssberg, The function of fillers in concrete, Mater. Struct. Constr. 37 (2004) 74–81. doi:10.1617/13694.

[14] H. Yanguatin, J. Tobón, J. Ramírez, Pozzolanic reactivity of kaolin clays , a review, 32 (2017) 13–24.

[15] V.M. Malhotra, P.K. Metha, Pozzolanic and Cementitious Materials, CRC Press - Taylor & Francis Group, 2017.

[16] A. Tironi, M.A. Trezza, A.N. Scian, E.F. Irassar, Assessment of pozzolanic activity of different calcined clays, Cem. Concr. Compos. 37 (2013) 319–327. doi:10.1016/j.cemconcomp.2013.01.002.

[17] S. Hollanders, R. Adriaens, J. Skibsted, Ö. Cizer, J. Elsen, Pozzolanic reactivity of pure calcined clays, Appl. Clay Sci. 132–133 (2016) 552–560. doi:10.1016/j.clay.2016.08.003.

[18] M.C.G. Juenger, R. Siddique, Recent advances in understanding the role of supplementary cementitious materials in concrete, Cem. Concr. Res. cli (2015) 71–80. doi:10.1016/j.cemconres.2015.03.018.

[19] F. Avet, X. Li, K. Scrivener, Determination of the amount of reacted metakaolin in calcined clay blends, Cem. Concr. Res. 106 (2018) 40–48. doi:10.1016/j.cemconres.2018.01.009.

[20] S. Seraj, R. Cano, R.D. Ferron, M.C.G. Juenger, The role of particle size on the performance of pumice as a supplementary cementitious material, Cem. Concr. Compos. 80 (2017) 135–142. doi:10.1016/j.cemconcomp.2017.03.009.

[21] E. John, T. Matschei, D. Stephan, Cement and Concrete Research Nucleation seeding with calcium silicate hydrate – A review, Cem. Concr. Res. 113 (2018) 74–85. doi:10.1016/j.cemconres.2018.07.003.

[22] T. Oey, A. Kumar, J.W. Bullard, N. Neithalath, G. Sant, The Filler Effect : The Influence of Filler Content and Surface Area on Cementitious Reaction Rates, 14th Int. Congr. Chem. Cem. (2015) 1–33.

[23] G.C. Cordeiro, R.D. Toledo Filho, L.M. Tavares, E.M.R. Fairbairn, Pozzolanic activity and filler effect of sugar cane bagasse ash in Portland cement and lime mortars, Cem. Concr. Compos. 30 (2008) 410–418. doi:10.1016/j.cemconcomp.2008.01.001.

[24] J. Tangpagasit, R. Cheerarot, C. Jaturapitakkul, K. Kiattikomol, Packing effect and pozzolanic reaction of fly ash in mortar, Cem. Concr. Res. 35 (2005) 1145–1151. doi:10.1016/j.cemconres.2004.09.030.

[25] I. Mehdipour, A. Kumar, K.H. Khayat, Rheology, hydration, and strength evolution of interground

494 limestone cement containing PCE dispersant and high volume supplementary cementitious materials,
495 Mater. Des. 127 (2017) 54–66. doi:10.1016/j.matdes.2017.04.061.
496 [26] K. De Weerdt, M. Ben Haha, G. Le Saout, K.O. Kjellsen, H. Justnes, B. Lothenbach, Hydration
497 mechanisms of ternary Portland cements containing limestone powder and fly ash, Cem. Concr. Res. 41
498 (2011) 279–291. doi:10.1016/j.cemconres.2010.11.014.
499 [27] V. Della, I. Kuhn, D. Hotza, Rice husk ash as an elemente source for active silicaproduction, Mater. Lett.
500 57 (2002) 818–821. doi:10.1016/S0167-577X(02)00879-0.
501 [28] N. Zemke, E. Woods, Rice Husk Ash, Rice Husk Ash. (2009) 1–12. http://www.cvbt-
502 web.org/uploads/Rice_Husk_Ash/Nick_Emmet_RHA.pdf.
503 [29] M.F.M. Zain, M.N. Islam, F. Mahmud, M. Jamil, Production of rice husk ash for use in concrete as a
504 supplementary cementitious material, Constr. Build. Mater. 25 (2011) 798–805.
505 doi:10.1016/j.conbuildmat.2010.07.003.
506 [30] R.S. Almenares, L.M. Vizcaíno, S. Damas, A. Mathieu, A. Alujas, F. Martirena, Industrial calcination of
507 kaolinitic clays to make reactive pozzolans, Case Stud. Constr. Mater. 6 (2017) 225–232.
508 doi:10.1016/j.cscm.2017.03.005.
509 [31] D. Zhou, R. Wang, M. Tyrer, H. Wong, C. Cheeseman, Sustainable infrastructure development through
510 use of calcined excavated waste clay as a supplementary cementitious material, J. Clean. Prod. 168
511 (2017) 1180–1192. doi:10.1016/j.jclepro.2017.09.098.
512 [32] R.D. Toledo Filho, J.P. Gonçalves, B.B. Americano, E.M.R. Fairbairn, Potential for use of crushed waste
513 calcined-clay brick as a supplementary cementitious material in Brazil, Cem. Concr. Res. 37 (2007)
514 1357–1365. doi:10.1016/j.cemconres.2007.06.005.
515 [33] L.R. Steiner, A.M. Bernardin, F. Pelisser, Effectiveness of ceramic tile polishing residues as
516 supplementary cementitious materials for cement mortars, Sustain. Mater. Technol. 4 (2015) 30–35.
517 doi:10.1016/j.susmat.2015.05.001.
518 [34] S. Wild, J.M. Khatib, O. M., Sulphate resistance of mortar, containing ground brick clay calcined at
519 different temperatures, 27 (1997) 697–709.
520 [35] L.A. Pereira-de-oliveira, J.P. Castro-gomes, P.M.S. Santos, The potential pozzolanic activity of glass and
521 red-clay ceramic waste as cement mortars components, Constr. Build. Mater. 31 (2012) 197–203.
522 doi:10.1016/j.conbuildmat.2011.12.110.

[36] Y. Labbaci, B. Labbaci, Y. Abdelaziz, A. Mekkaoui, A. Alouani, The use of the volcanic powders as supplementary cementitious materials for environmental-friendly durable concrete, Constr. Build. Mater. 133 (2017) 468–481. doi:10.1016/j.conbuildmat.2016.12.088.

[37] A. Ababneh, F. Matalkah, Potential use of Jordanian volcanic tuffs as supplementary cementitious materials, Case Stud. Constr. Mater. 8 (2018) 193–202. doi:10.1016/j.cscm.2018.02.004.

[38] W.Y. Kuo, J.S. Huang, T.E. Tan, Organo-modified reservoir sludge as fine aggregates in cement mortars, Constr. Build. Mater. 21 (2007) 609–615. doi:10.1016/j.conbuildmat.2005.12.009.

[39] O. Rodríguez, L. Kacimi, A. López-delgado, M. Frías, A. Guerrero, Characterization of Algerian reservoir sludges for use as active additions in cement : New pozzolans for eco-cement manufacture, 40 (2013) 275–279. doi:10.1016/j.conbuildmat.2012.10.016.

[40] V.B. Thapa, D. Waldmann, J.-F. Wagner, A. Lecomte, Assessment of the suitability of gravel wash mud as raw material for the synthesis of an alkali-activated binder, Appl. Clay Sci. 161 (2018) 110–118. doi:10.1016/j.clay.2018.04.025.

[41] Ł. Kotwica, W. Pichór, E. Kapeluszna, A. Różycka, Utilization of waste expanded perlite as new effective supplementary cementitious material, J. Clean. Prod. 140 (2017) 1344–1352. doi:10.1016/j.jclepro.2016.10.018.

[42] E. Aprianti S, A huge number of artificial waste material can be supplementary cementitious material (SCM) for concrete production – a review part II, J. Clean. Prod. 142 (2017) 4178–4194. doi:10.1016/j.jclepro.2015.12.115.

[43] E. Aprianti, P. Shafigh, S. Bahri, J.N. Farahani, Supplementary cementitious materials origin from agricultural wastes - A review, Constr. Build. Mater. 74 (2015) 176–187. doi:10.1016/j.conbuildmat.2014.10.010.

[44] J.M. Paris, J.G. Roessler, C.C. Ferraro, H.D. Deford, T.G. Townsend, A review of waste products utilized as supplements to Portland cement in concrete, J. Clean. Prod. 121 (2016) 1–18. doi:10.1016/j.jclepro.2016.02.013.

[45] G. Quercia, J.J.G. Van Der Putten, G. Hüsken, H.J.H. Brouwers, Photovoltaic's silica-rich waste sludge as supplementary cementitious material (SCM), Cem. Concr. Res. 54 (2013) 161–179. doi:10.1016/j.cemconres.2013.08.010.

[46] P.F.G. Banfill, Alternative materials for concrete- Mersey silt as fine aggregate, Build. Environ. 15 (1980) 181–190. doi:10.1016/0360-1323(80)90035-9.

[47] DIN EN 197-1:2011-11, Cement - Part 1: Composition, specifications and conformity criteria for common cements, European Committee for standardization, 2011.

[48] DIN EN 196-1:2016-11, Methods of Testing Cement - Part 1: Determination of Strength, European Committee for standardization, 2016.

[49] R.W. Cheary, A.A. Coelho, J.P. Cline, Fundamental parameters line profile fitting in laboratory diffractometers, 109 (2004) 1–25. doi:10.6028/jres.002.

[50] H.M. Rietveld, A profile refinement method for nuclear and magnetic structures, J. Appl. Crystallogr. 2 (1969) 65–71. doi:10.1107/S0021889869006558.

[51] A.H. De Aza, A.G. De La Torre, M.A.G. Aranda, F.J. Valle, S. De Aza, Rietveld Quantitative Analysis of Buen Retiro Porcelains, 87 (2004) 449–454. doi:10.1111/j.1551-2916.2004.00449.x.

[52] C. Jaturapitakkul, K. Kiattikomol, S. Songpiriyakij, A Study of Strength Activity Index of Ground Coarse Fly Ash with Portland Cement, Sci. Asia. 25 (1999) 223–229.

[53] Y. Liu, S. Lei, M. Lin, Y. Li, Z. Ye, Y. Fan, Assessment of pozzolanic activity of calcined coal-series kaolin, Appl. Clay Sci. 143 (2017) 159–167. doi:10.1016/j.clay.2017.03.038.

[54] Y. Shao, T. Lefort, S. Moras, D. Rodriguez, Studies on concrete containing ground waste glass, Cem. Concr. Res. 30 (2000) 91–100. doi:10.1016/S0008-8846(99)00213-6.

[55] A. Shvarzman, K. Kovler, G.S. Grader, G.E. Shter, The effect of dehydroxylation / amorphization degree on pozzolanic activity of kaolinite, 33 (2003) 405–416. doi:10.1016/S0008-8846(02)00975-4.

[56] C. Shi, Y. Wu, C. Riefler, H. Wang, Characteristics and pozzolanic reactivity of glass powders, Cem. Concr. Res. 35 (2005) 987–993. doi:10.1016/j.cemconres.2004.05.015.

[57] A. Bakolas, E. Aggelakopoulou, A. Moropoulou, Evaluation of pozzolanic activity and physico-mechanical characteristics in ceramic powder-lime pastes, J. Therm. Anal. Calorim. 84 (2006) 157–163. doi:10.1007/s10973-007-8858-1.

[58] S. Donatello, M. Tyrer, C.R. Cheeseman, Comparison of test methods to assess pozzolanic activity, Cem. Concr. Compos. 32 (2010) 121–127. doi:10.1016/j.cemconcomp.2009.10.008.

[59] D.P. Bentz, A. Durán-Herrera, D. Galvez-Moreno, Comparison of ASTM C311 Strength Activity Index Testing versus Testing Based on Constant Volumetric Proportions, J. ASTM Int. 9 (2012) 104138.

580 doi:10.1520/JAI104138.
581 [60] A. Tironi, M.A. Trezza, A.N. Scian, E.F. Irassar, Kaolinitic calcined clays: Factors affecting its
582 performance as pozzolans, Constr. Build. Mater. 28 (2012) 276–281.
583 doi:10.1016/j.conbuildmat.2011.08.064.
584 [61] A. Tironi, F. Cravero, A.N. Scian, E.F. Irassar, Pozzolanic activity of calcined halloysite-rich kaolinitic
585 clays, Appl. Clay Sci. 147 (2017) 11–18. doi:10.1016/j.clay.2017.07.018.
586 [62] R.L. Coble, Effects of particle-size distribution in initial-stage sintering, J. Am. Ceram. Soc. 56 (1973)
587 461–466.
588 [63] V.-G. Lee, T.-H. Yeh, Sintering effects on the development of mechanical properties of fired clay
589 ceramics, Mater. Sci. Eng. A. 485 (2008) 5–13.
590 [64] Paul, M. (2018). Quality control of autoclaved aerated concrete by means of X-ray diffraction. ce/papers,
591 2(4), 111-116. doi.org/10.1002/cepa.894.
592 [65] B. Wunderlich, Thermal analysis of polymeric materials, Springer Science & Business Media, 2005.
593 doi:10.1520/C0618-12A.
594 [66] R.C. Mielenz, N.C. Schieltz, M.E. King, Thermogravimetric analysis of clay and clay-like minerals, Clay
595 Clay Miner. (1953) 285–314.
596 [67] ASTM C618-12a, Standard Specification for Coal Fly Ash and Raw or Calcined Natural Pozzolan for
597 Use in Concrete, ASTM International.
598 [68] ASTM C311-05, Standard Test Methods for Sampling and Testing Fly Ash or Natural Pozzolans for Use
599 in Portland-Cement Concrete, 2004. doi:10.1520/C0311-05.
600 [69] S. Ferreiro, M.M.C. Canut, J. Lund, D. Herfort, Influence of fineness of raw clay and calcination
601 temperature on the performance of calcined clay-limestone blended cements, Appl. Clay Sci. 169 (2019)
602 81–90. doi:10.1016/J.CLAY.2018.12.021.